Robustness of Downhill Folding: Guidelines for the Analysis of Equilibrium Folding Experiments on Small Proteins

Athi N. Naganathan,[†,‡] Raúl Perez-Jimenez,[†,§] Jose M. Sanchez-Ruiz,[*,§] and Victor Muñoz[*,‡]

Department of Chemistry and Biochemistry, and Center for Biomolecular Structure and Organization, University of Maryland, College Park, Maryland 20742, and Departamento de Química-Física, Facultad de Ciencias, Universidad de Granada, Granada 18071, Spain

Received January 20, 2005; Revised Manuscript Received March 23, 2005

ABSTRACT: Previously, we identified the protein BBL as a downhill folder. This conclusion was based on the statistical mechanical analysis of equilibrium experiments performed in two variants of BBL, one with a fluorescent label at the N-terminus, and another one labeled at both ends. A recent report has claimed that our results are an artifact of label-induced aggregation and that BBL with no fluorescent labels and a longer N-terminal tail folds in a two-state fashion. Here, we show that singly and doubly labeled BBL do not aggregate, unfold reversibly, and have the same thermodynamic properties when studied under appropriate experimental conditions (e.g., our original conditions (*1*)). With an elementary analysis of the available data on the nonlabeled BBL (*2*), we also show that this slightly more stable BBL variant is not a two-state folder. We discuss the problems that led to its previous misclassification and how they can be avoided. Finally, we investigate the equilibrium unfolding of the singly labeled BBL with both ends protected by acetylation and amidation. This variant has the same thermodynamic stability of the nonlabeled BBL and displays all the equilibrium signatures of downhill folding. From all these observations, we conclude that fluorescent labels do not perturb the thermodynamic properties of BBL, which consistently folds downhill regardless of its stability and specific protein tails. The work on BBL illustrates the shortcomings of applying conventional procedures intended to distinguish between two-state and three-state folding models to small fast-folding proteins.

It has been realized for decades that protein folding cannot occur by protein molecules randomly sampling all of their available conformational space (*3*). More recently, theory (*4*−*13*) has provided a simple explanation for the force driving the folding process. The basic underlying idea is that as the protein molecule increases its nativeness, it also progressively lowers its average interaction energy (*5*, *8*). This factor provides an energy gradient that effectively guides the protein molecule toward the native structure in its motion through a hyperdimensional conformational space. The projection of the hyperdimensional surface into a few order parameters results in a free-energy surface with shape determined by the precise balance between the decrease in interaction energy (i.e., including solvent interactions) and the opposing decrease in conformational entropy (*5*). In the simplest case, and depending on the energy bias toward the native state, the projected free energy presents either a barrier separating two minima or a downhill surface with just one minimum. These two situations correspond, respectively, to the scenario 1 and scenario 0 of the energy landscape approach to protein folding (*5*). Therefore, the effective free-energy barrier (defined as the free-energy difference between the shallower minimum and the maximum of the lowest free-energy path) is expected to be maximal at the midpoint of the folding transition and to decrease at higher and lower native biases. A direct manifestation of this behavior is found in the typical V-shaped plot of the folding relaxation time as a function of chemical denaturant concentration (*14*).

Theory provides the general principle, but the details defining the specific shape of the free-energy surface should strongly depend on the three-dimensional structure and amino acid sequence of the protein. Most single domain proteins that have been experimentally studied to date seem to fold crossing a free-energy barrier (*15*). However, for some of these proteins, the barrier is not very high (i.e., a few kcal/mol) (*16*). Furthermore, such small barriers can be further reduced, or even eliminated, by artificially strengthening the bias toward the native state with mutations and cosolvents, as it has been recently shown for monomeric λ repressor (*17*, *18*).

In the spirit of the theoretical description given above, one of us proposed that for some proteins the balance between interaction energy and conformational entropy could result in a free-energy surface that displays only one minimum at all degrees of native bias (*19*). The only minimum shifts progressively from native to unfolded values as the native bias is reduced (e.g.. by increasing temperature). In a free-energy surface with only one minimum, the dynamics are always going in favor of the gradient, and the folding−unfolding relaxation is globally downhill. An important

* Corresponding authors. V.M.: phone, (301) 405-3165; fax, (301) 314-0286; e-mail, vm48@umail.umd.edu. J.M.S.-R.: phone, (34) 958-243189; fax, (34) 958-272879; email, sanchezr@ugr.es.

[†] These two authors have contributed equally to this work.

[‡] University of Maryland.

[§] Universidad de Granada.

10.1021/bi050118y CCC: $30.25
Published on Web 04/27/2005

Naf-BBL: NH_3^+-NafA-LSPAIRRLLAEHNLDASAIKGTGVGGRLTREDVEKHLAK-COO^-

Naf-BBL-Dan: NH_3^+-NafA-LSPAIRRLLAEHNLDASAIKGTGVGGRLTREDVEKHLA-DanK-COO^-

QNND-BBL: NH_3^+-QNNDALSPAIRRLLAEHNLDASAIKGTGVGGRLTREDVEKHLAK-COO^-

Ac-Naf-BBL-NH_2: CH_3CONH-NafA-LSPAIRRLLAEHNLDASAIKGTGVGGRLTREDVEKHLAK-$CONH_2$

FIGURE 1: Sequences and names of the four BBL variants. NafA, naphthyl-alanine; DanK, dansyl-lysine; Ac, acetyl.

implication of the global downhill regime is that it results in signature thermodynamic behavior. The reason is that the free-energy surface is barrierless throughout the complete unfolding process, so that the equilibrium transition is continuous instead of first-order. Thus, global downhill folding can be detected in equilibrium experiments (*1*, *19*). This contrasts with situations in which the free-energy barrier disappears only at extreme conditions of native bias (i.e., strongly stabilizing and strongly destabilizing), which might be inaccessible to experiment or require fast time-resolved measurements.

On the basis of these ideas, we reported that the small helical protein BBL is a global downhill folder. We reached this conclusion by studying the equilibrium thermal unfolding of BBL with several spectroscopic techniques and differential scanning calorimetry (DSC) and by analyzing the results with an elementary statistical mechanical model. We later confirmed the downhill character of BBL by investigating the coupling between temperature and chemical denaturation in BBL (*20*) and by analyzing the DSC experiments with a variable-barrier phenomenological model based on Landau's theory of critical transitions (*21*). The experiments described in these previous works were performed in a protein encompassing residues 111 to 150 of *Escherichia coli*'s E2 chain of the 2-oxoglutarate dehydrogenase complex, in which alanine 111 was substituted by naftyl-alanine to incorporate a fluorescent probe (hereafter termed Naf-BBL, see Figure 1). For the FRET and intrinsic fluorescence measurements, we also employed a variant of BBL with two fluorescent probes: the N-terminal naphthyl-alanine and a dansyl-lysine in position 150 (hereafter termed Naf-BBL-Dan, see Figure 1). Naf-BBL-Dan showed a tendency to aggregate at pH 7, but in experiments carried out at low-protein and -salt concentration, its thermal unfolding transition monitored by circular dichroism was reversible and identical to that of Naf-BBL (*1*). Both of these proteins were chemically synthesized with the ends free.

Very recently, Fersht and co-workers have reported an investigation of the equilibrium unfolding behavior of another variant of BBL (*2*). Their BBL variant incorporates four additional N-terminal residues that belong to an unstructured tail (*22*), has no fluorescent labels, and has been produced by recombinant means (hereafter termed QNND-BBL, see Figure 1). Fersht and co-workers find that QNND-BBL is slightly more stable than our BBL variants (maximum of DSC thermogram is shifted ~8 K higher) and conclude that QNND-BBL is a two-state folder. Their manuscript also includes data on Naf-BBL-Dan. However, the results reported therein are not relevant to the folding behavior of this protein because their experiments were performed under conditions that we had previously reported to be conducive to aggregation (*1*).

The work of Fersht and co-workers provides an opportunity to compare experimental data from different groups and to investigate the effect of the protein tails on the thermodynamic properties of BBL. Perhaps even more importantly, their work creates the perfect setting for a much needed discussion on the analysis of equilibrium experimental data in protein folding. Folding reactions have been traditionally interpreted in the context of two-state and three-state chemical models. Along these lines, the observation of sigmoidal unfolding curves and single-peaked DSC thermograms has often been seen as indicative of a two-state transition (*2*). However, these criteria are inappropriate to distinguish between first-order and continuous transitions. Indeed, recent theoretical analyses with elementary statistical mechanical (*1*, *20*) and polymer-chain models (*23*) show that sigmoidal curves and single-peaked DSC curves are also present in barrierless unfolding transitions such as the ones we observe in our BBL variants. Such realization highlights the importance of redefining the procedures and criteria for the analysis of experimental data in protein folding. This is even more critical when investigating the characteristically broad unfolding transitions of small fast-folding proteins.

Here, we attempt to do just that. We start by introducing experimental data showing that the unfolding of both, Naf-BBL and Naf-BBL-Dan, is reversible and with the same thermodynamic properties. We continue with an elementary analysis of Fersht and co-workers's experiments on QNND-BBL. Such analysis unambiguously indicates that QNND-BBL does not fold in a two-state manner. In fact, QNND-BBL appears to share the overall folding behavior of our original BBL variants, but with higher stability. We also investigate the equilibrium unfolding of yet another variant of BBL. This variant is identical to Naf-BBL but has the end-charges removed by acetylation of the N-terminus and amidation of the C-terminus (hereafter termed Ac-Naf-BBL-NH_2, see Figure 1). We find that the stability and general thermodynamic properties of this protein are the same as those previously reported by Fersht and co-workers for QNND-BBL. Therefore, the slight difference in stability between our original BBL variants and QNND-BBL seems to arise from repulsive interactions between the N-terminal charge and the macrodipole of helix 1. Furthermore, these results exemplify that the fluorescent probes that we have used do not perturb the folding of BBL to any significant degree. Finally, we show that the equilibrium unfolding of Ac-Naf-BBL-NH_2 displays all the equilibrium signatures for downhill folding, including signatures based on the coupling between temperature and chemical denaturation (*20*) and on the analysis of calorimetric data (*21*). From all of these observations, we conclude that downhill folding is a robust property of BBL.

MATERIALS AND METHODS

Protein Synthesis. Protein synthesis, purification, and analysis for Naf-BBL, Naf-BBL-Dan, and Ac-Naf-BBL-NH_2 was carried out as described in Garcia-Mira et al. (*1*).

Calorimetry. DSC experiments were carried out with a VP-DSC calorimeter from MicroCal (Northhamton, MA) at a scan-rate of 1.5 K/min. Protein solutions for the calorimetric experiments were prepared by exhaustive dialysis against the buffer. Calorimetric cells (operating volume ~0.5 mL) were kept under an excess pressure of 30 psi to prevent degassing during the scan. In all measurements, the buffer from the last dialysis step was used in the reference cell of the calorimeter. Several buffer−buffer baselines were obtained before each protein run to ascertain proper equilibration of the instrument. In most experiments, one or several reheating runs were carried out to determine the reversibility of the denaturation process. Finally, an additional buffer−buffer baseline was obtained immediately after the protein runs to rule out significant changes in instrumental baseline. The level of instrumental baseline reproducibility attained was very high (see inset in Figure 2A). For each protein, three independent DSC experiments were carried out under the same buffer conditions but with different protein concentrations within the 0.2−0.8 mg/mL range. Absolute heat capacity values and their associated errors were calculated from the protein concentration dependence of the apparent heat capacities, as described in ref *24*.

Far-UV Circular Dichroism. Circular dichroism (CD) experiments and sample preparation were carried out as described in Oliva and Muñoz (*20*). The concentrations of Naf-BBL and Ac-Naf-BBL-NH_2 were measured at the maximum absorption wavelength of naphthyl-alanine (280 nm; $\epsilon_{280} = 5526\ M^{-1}\ cm^{-1}$) using a Hewlett-Packard 8452A Diode Array Spectrophotometer. Concentration of Naf-BBL-Dan was determined by taking an average of the concentrations determined at two wavelengths: 280 and 266 nm (which is a pH-independent isosbestic point for dansyl). The molar extinction coefficients used were 1571 and 4528 $M^{-1}\ cm^{-1}$ for dansyl, 5526 and 3595 $M^{-1}\ cm^{-1}$ for naphthyl, at 280 and 266 nm, respectively. CD spectra of Naf-BBL-Dan at low-protein concentration were measured reducing the scanning speed to 5 nm/min with 32 s response time to increase the signal-to-noise ratio. The reversibility of the unfolding transition was routinely checked comparing pre- and postunfolding CD spectra at 298 K. All urea−temperature denaturation experiments for Ac-Naf-BBL-NH_2 were performed as described in Oliva and Muñoz (*20*) for Naf-BBL. The previous urea denaturation data for Naf-BBL at 298 K (*20*) were extended to 9 M urea in steps of 0.5 M. Urea concentrations were measured directly by refractometry.

Data Analysis and Fitting Procedures. All of the data on QNND-BBL were extracted from ref *2* using DigitizeIt 1.5.7. The DSC data for QNND-BBL were fitted to two-state models as described in the text. To estimate possible digitization errors, we carried out three independent digitization rounds. Two-state fits to each of the three digitized datasets produced thermodynamic parameters, T_m and ΔH_m, that agreed within 0.04 K and 0.8 kJ/mol, respectively. The digitized NMR data for QNND-BBL were normalized to the values at the highest and lowest common temperatures and fitted to two-state models (the digitization error in the temperature scale was ~0.06 K) using a fixed value for ΔC_p of 1.67 kJ/(mol·K) to reproduce the fits of ref *2*. A simple error analysis was performed to quantify the effect of white noise in the fitting procedure. Statistical noise of magnitude equal to the experimental noise was added to a noise-free reference curve (i.e., a theoretical curve calculated with a two-state model). Two-state fits were then performed: (i) fixing the thermodynamic parameters (ΔH_m and T_m) to their true values, and (ii) allowing all the parameters to float. DSC data for Naf-BBL and Ac-Naf-BBL-NH_2 were fitted to two-state models with linear baselines for the native and unfolded state (two parameters each). All fits resulted in the crossing of baselines. Similar results were obtained when the slope for the folded baseline was fixed or when the change in heat capacity between the two-states (ΔC_p) was fixed. The urea−temperature unfolding CD data of Naf-BBL and Ac-Naf-BBL-NH_2 were fitted to global two-state models in which ΔH and ΔS were assumed to change linearly with urea, and ΔC_p was assumed constant. Linear dependences of ΔH and ΔS with urea and very small changes in ΔC_p with urea have been reported by Felitsky and Record in lac-repressor (*25*). This fitting procedure differs from the global two-state fits described in Oliva and Muñoz (*20*), in which Schellman's solvent-exchange model (*26*) was used to describe the coupling between temperature and urea. Here, we have used the simpler linear extrapolation model to facilitate comparison with the parameters available in the literature for other proteins. The native baseline was assumed to be linearly dependent on temperature and independent of urea. The unfolded baseline required five parameters: quadratic dependence on temperature, linear dependence on urea, and a coupling parameter between the two denaturing agents. The global fit included a total of 13 adjustable parameters with ΔH_m, T_m, ΔC_p, urea dependence of ΔS, and ΔH being the remainder. Individual two-state fits were performed as explained in the text.

RESULTS AND DISCUSSION

Singly and Doubly Labeled BBL Unfold Reversibly and with the Same Thermodynamic Properties. Naf-BBL showed no tendency to aggregate in any of the conditions that we have tested, including protein concentrations up in the millimolar range. The analysis with differential scanning calorimetry (DSC) reveals that the equilibrium thermal unfolding of this protein is extremely reversible. Figure 2A shows the raw DSC thermograms of a series of four heating−cooling scans of Naf-BBL after baseline subtraction. The inset shows the reproducibility of the instrumental baseline in the experiment. The difference in heat capacity between the maximum of the thermogram (i.e., ~324 K) and the values at high temperature is within 5% for all the scans. Furthermore, there is no indication of any decrease in the amplitude throughout multiple scans, as would accompany aggregation or any other irreversible phenomena. During the first heating of the sample, a small artifact is reproducibly observed at low temperatures (see Figure 2A). This artifact probably reflects reversible structural changes induced by the dehydration−lyophilization of our chemically synthesized samples, as it has been reported for several proteins by Klibanov and co-workers (*27*, *28*). Here, as we have done in our previous work (*1*), we use the second DSC scan to minimize errors in the determination of the heat capacity at low temperatures.

In contrast to the behavior of Naf-BBL, the incorporation of the dansyl group at the C-terminus produces a significant increase in the tendency of Naf-BBL-Dan to aggregate (*1*). Aggregation of this protein is easily detected from the

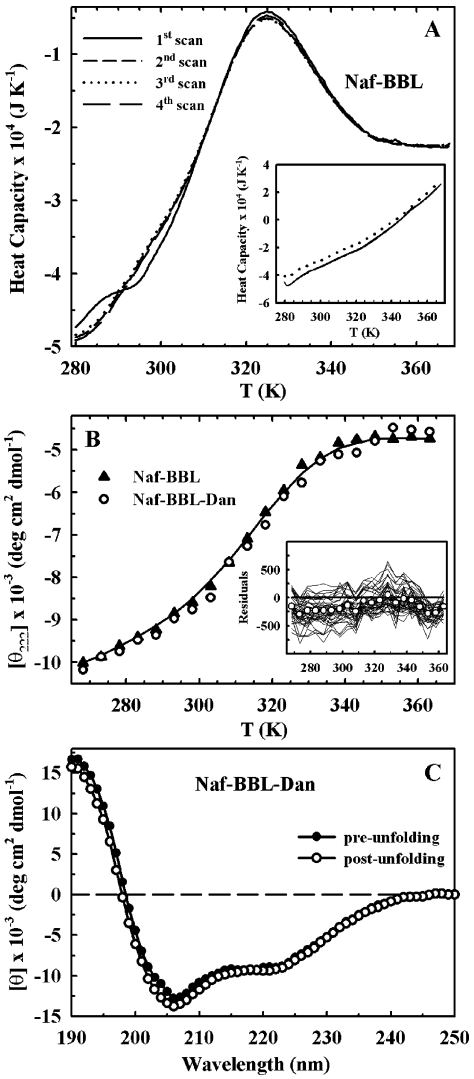

FIGURE 2: (A) Reversibility of Naf-BBL thermal unfolding monitored by DSC. Thermograms are shown in raw heat capacity units and baseline corrected. (inset) Baseline reproducibility; (continuous lines) six subsequent baselines measured before measuring the protein, (dotted line) baseline upon refilling the calorimeter after the protein scan. (B) Thermal unfolding curves for Naf-BBL at 50 μM protein concentration (triangles) and Naf-BBL-Dan at 12.7 μM protein concentration (circles) measured by CD at 222 nm in buffer phosphate 5mM, pH 7. The continuous line is shown to guide the eye. (inset) Residuals between the data for Naf-BBL-Dan and Naf-BBL for different wavelengths. The circles represent the wavelength-averaged residuals. (C) Far-UV CD spectrum of Naf-BBL-Dan at 298 K measured before (filled circles) and after (open circles) thermal denaturation.

emergence of any or all of the following signs: (i) a DSC thermogram with an exothermic peak that depends on protein concentration, (ii) irreversible blue-shifts in the emission maximum of the dansyl group, and (iii) thermal unfolding transitions monitored by far-UV circular dichroism (CD) that are irreversible and become broader as protein concentration is increased. In addition to the expedient solution of decreasing protein concentration, aggregation of Naf-BBL-Dan can be greatly reduced by decreasing ionic strength and/or pH. At pH 7.0, low ionic strength (i.e., $\leq$20 mM buffer phosphate), and protein concentrations lower than 25 μM (e.g., the conditions used in our original report (*1*)), the thermal unfolding transition of Naf-BBL-Dan is reversible and identical to that of Naf-BBL. Figure 2B shows the thermal unfolding transition of Naf-BBL-Dan under such conditions as monitored by the CD signal at 222 nm. The thermal unfolding transition of 50 μM Naf-BBL measured at the same pH and ionic strength is also shown for comparison. The inset shows the residuals between the CD signals of Naf-BBL and Naf-BBL-Dan at the different wavelengths, together with the wavelength-averaged residuals. The data of Naf-BBL-Dan is noisier because it has been obtained at lower protein concentrations. However, the small magnitude and lack of any apparent trend in the residuals indicate that the CD spectrum of these two BBL variants is essentially the same at all of the temperatures explored. The reversibility of the Naf-BBL-Dan unfolding is shown in Figure 2C, which displays the CD spectrum of Naf-BBL-Dan before and after the complete thermal unfolding experiment of Figure 2B.

To illustrate the agreement between the thermodynamic properties of Naf-BBL and Naf-BBL-Dan, we used a two-state analysis of the CD thermal denaturation profiles. Such two-state analysis is not physically meaningful for these proteins, but it still provides a simple common ground to compare the two transitions quantitatively. The simplest possible two-state analysis (i.e., neglecting the temperature dependence of ΔH and ΔS within the transition region) of the 222 nm CD data for Naf-BBL produces a good fit with $\Delta H_m = 91$ kJ/mol and $T_m = 321$ K. Fitting the unfolding transition of Naf-BBL-Dan by letting the two baselines and their slopes float, but constraining the values of ΔH_m and T_m to those obtained for Naf-BBL, produces a fit with a sum of least squares (SLS) that is only 9% higher than the SLS of its best unconstrained fit. An increase in SLS of 9% is actually lower than the 20% average increase expected if the discrepancy between the two sets of parameters is only due to experimental noise. The statistically expected increase in SLS was easily estimated from theoretically generated two-state curves to which statistical noise was added to match the magnitude of the observed experimental noise. Fitting of such two-state curves with ΔH_m and T_m constrained to their true values (i.e., four adjustable parameters) rendered SLSs that were on average 20% higher than those of fully unconstrained fits (i.e., six adjustable parameters). Thus, the statistical analysis indicates that, within the precision of the experimental data, the thermodynamic parameters of Naf-BBL and Naf-BBL-Dan are identical. At a more qualitative level, the same conclusion can be reached from a visual inspection of Figure 2B. Naf-BBL-Dan has also been recently used to measure the relaxation dynamics of protein hydrophobic collapse (*29*). For this purpose, experiments were carried out in acidic conditions, which reduce the aggregation propensity of Naf-BBL-Dan and allow the use of much higher protein concentrations.

Elementary Analysis Shows that QNND-BBL Is Not a Two-State Folder. The equilibrium folding behavior of QNND-BBL has recently been investigated by Fersht and co-workers (*2*). These authors reported that the thermodynamic properties of QNND-BBL are different to those of Naf-BBL and Naf-BBL-Dan and concluded that QNND-BBL folds in a two-state manner (*2*). In this section, we analyze the experimental data of Fersht and co-workers on QNND-BBL to ascertain

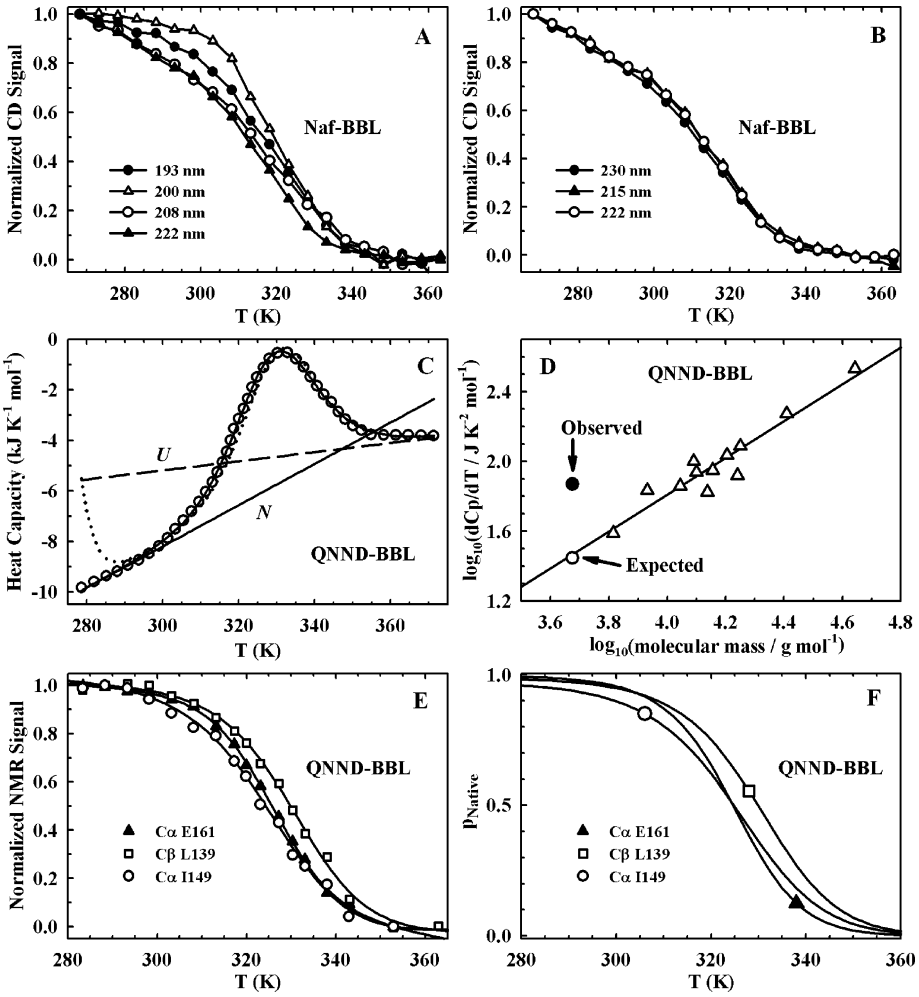

FIGURE 3: (A) Normalized thermal unfolding transitions of Naf-BBL monitored by CD at the wavelengths used in Garcia-Mira et al. (*1*). (B) Normalized thermal unfolding transitions of Naf-BBL monitored by CD at the wavelengths used by Fersht and co-workers (*2*). (C) DSC thermogram of QNND-BBL: (circles) data of Fersht and co-workers (*2*), (continuous curve) fit to a two-state model enforcing a $\Delta H_{cal}/\Delta H_{vH}$ of unity, (straight lines) "native" and "unfolded" fitting baselines, and (dotted curve) thermogram predicted by calculating ΔC_p from baselines. (D) Empirical correlation between dC_p/dT and molecular mass: (triangles) experimental data from the 12 proteins originally used in Freire's correlation (*36*), (open circle) estimation for QNND-BBL, (filled circle) measured for QNND-BBL from the 280−300 K data in C. (E) Normalized ^{13}C chemical shifts as a function of temperature of several atoms of QNND-BBL as measured by Fersht and co-workers (*2*). The continuous lines are fits to independent two-state models. (F) QNND-BBL native state probabilities calculated from the fits shown in panel E.

whether this protein is indeed a two-state folder or rather has more complex conformational behavior.

One of the experimental signs that the equilibrium folding transition of a protein is not two-state is the observation of apparent thermal unfolding transitions that change when monitoring different structural features (*1*, *19*). In proteins composed of α-helices and coil segments, the far-UV CD spectrum alone offers a particularly simple means of investigating the structural heterogeneity of the unfolding transition. The reason is that the shape of the α-helical CD spectrum depends on the length and straightness of the α-helix. This is a consequence of exciton effects arising from the multiple alignment of peptide−bond dipoles with the α-helix axis (*30*). The spectral changes mainly affect the relative intensity of the α-helical bands at 193, 208, and 222 nm (*31*). In our original report of downhill folding, we used this effect to demonstrate that the apparent thermal unfolding transition of Naf-BBL (and Naf-BBL-Dan) is structurally complex (*1*). Indeed, the normalized thermal unfolding transition of these two proteins varies when observed at 193, 200, 208, and 222 nm (Figure 3A). The 193, 208, and 222 nm wavelengths report on each of the three α-helical bands, while 200 nm is a wavelength dominated by the changes in the coil signal. The transitions shown in Figure 3A reflect that the changes mostly occur in the pretransition slope and the apparent T_m and indicate that the α-helix CD spectrum is changing throughout the whole range of temperatures.

In their investigation of the folding behavior of QNND-BBL, Fersht and co-workers also measured the CD unfolding transition of this protein at several wavelengths. They report that all wavelengths give rise to the same normalized equilibrium thermal unfolding curves and argue that such coincidence demonstrates the two-state folding of QNND-BBL (*2*). The wavelengths employed by Fersht and co-workers range from 215 to 230 nm. Therefore, these wavelengths are different to the wavelengths that we originally employed (*1*). At first, this difference might seem an inconsequential detail, but it turns out to be a critical issue. In a protein with just α-helices and coil segments such as BBL, the 215−230 nm range of the CD spectrum reports almost entirely on just one of the three α-helical bands (i.e., the 222 band). Thus, measuring the CD thermal unfolding

of QNND-BBL within the 215−230 wavelength range *guarantees* obtaining similar thermal unfolding transitions for all of the experiments. This statement is demonstrated in Figure 3B, which shows that the normalized apparent thermal unfolding transition of the downhill folder Naf-BBL is also identical when monitored by CD at 230, 222, and 215 nm. The basic argument regarding the CD spectrum can be generalized to other conventionally used spectroscopic probes of folding. For example, it would be unlikely to observe differences in the unfolding transition of a protein when monitored by fluorescence, absorbance, near-UV CD, and NMR of a single chromophore, even if the folding behavior of the protein is not two-state. Although the range of wavelengths chosen by Fersht and co-workers severely restricts the information that can be obtained from their CD data, it is still possible to compare the magnitude of the CD pretransition temperature dependence. We previously reported that a pretransition CD signal that is highly sloped toward more disorder (i.e., less α-helix content for BBL variants) is another indication of structurally heterogeneous unfolding transitions (*20*). Interestingly, the normalized CD (222 nm) unfolding transitions of Naf-BBL and QNND-BBL have very similar pretransition slopes (normalization is required because the CD data for QNND-BBL is available only in raw ellipticity units (*2*)) (see Figure 4B).

The analysis of the DSC thermogram can also provide very important information regarding the two-stateness of the protein. In fact, we have recently shown that it is possible to directly estimate the height of the thermodynamic folding barrier of a protein from DSC data alone (*21*). Fersht and co-workers included DSC as part of their investigation of QNND-BBL folding (Figure 3C). One of the important properties of the DSC experiment is that the pre- and posttransition baselines give direct information about the magnitude of the enthalpy fluctuations in the low- and high-temperature ensembles. In a two-state analysis, these baselines correspond to the fluctuations in the native and unfolded states, and the difference between the two baselines determines the ΔC_p of unfolding (*32*−*35*). Freire and co-workers have shown that the heat capacity of the native state and its dependence with temperature (dC_p/dT) strongly correlate with the size of the protein ((*36*), Figure 3D). These linear correlations provide a basis for assessing the nativeness of the low-temperature baseline in a DSC thermogram. Naf-BBL displays values for both parameters that indicate the presence of enthalpy fluctuations that are too large for a unique native state (see Figure 4E). Previously, Dragan and Privalov made the same observations in a leucine zipper, and also interpreted them as indicative of non-two-state folding (*37*). The DSC data of QNND-BBL was not reported in absolute heat capacity units, as is obvious from the negative heat capacity scale (see Figure 3C). This fact eliminates the possibility of comparing their baseline with the values expected for a native protein. However, it is still possible to measure dC_p/dT from their data below 300 K. Such calculation renders a value of $\sim$74 J·K^{-2}·mol^{-1}, which corresponds to a native protein of $\sim$11.5 kDa instead of the 4.7 kDa QNND-BBL (Figure 3D). In fact, the slope measured for QNND-BBL is even higher than the slope of Naf-BBL (i.e., $\sim$55 J·K^{-2}·mol^{-1}). The result of this elementary calculation is in stark contrast with Fersht and co-workers's statement indicating that their pretransition DSC baseline displays only weak temperature dependence (*2*). The extremely high slope at low temperatures reported for QNND-BBL suggests the existence of very large fluctuations in its "native" state and, possibly, their coexistence with an experimental artifact (see next section).

The analysis of the DSC thermogram of QNND-BBL with a two-state model has been presented as further evidence supporting the two-state folding of this protein (*2*). The case has been primarily argued on the basis of the good agreement that was obtained between calorimetric (ΔH_{cal}) and van't Hoff (ΔH_{vH}) enthalpies of folding (*2*). A ratio between these two parameters close to unity has been traditionally seen as strong evidence of two-state-like behavior (*38*). This criterion is usually based on an analysis of the DSC thermogram in which the temperature dependence of ΔH and ΔS is neglected within the narrow range of temperatures covering the unfolding transition region. The thermogram is then fitted to a pseudo-two-state model with two different enthalpies: ΔH_{vH} determines the changes in the probability of native and unfolded states with temperature (i.e., it determines the broadness of the transition) and ΔH_{cal} determines the area over a chemical baseline that smoothly connects the pre- and posttransition baselines (which oftentimes are fitting parameters themselves). If these two enthalpies converge to the same value, the implication is that the two-state assumption holds. However, this criterion by itself is not sufficient without further evaluation of the baselines obtained in the fit. Baseline evaluation was amply discussed in the early calorimetric studies of protein unfolding (*38*). It is of particular importance if the calorimetric transition is broad, as is typically observed for small proteins. This is because the fitting procedure can choose calorimetric baselines that largely trim the wings of the excess heat capacity curve thereby eliminating data that might be incompatible with a two-state model. The critical effect of baseline trimming was first addressed by Karplus and collaborators who showed that theoretical DSC curves calculated with a three-state model could be fit to a two-state model by choosing suitable baselines (*39*). Using polymer-chain models, Kaya and Chan have subsequently generalized the consequences of baseline trimming to situations more akin to those encountered in protein denaturation experiments (*40*). In fitting experimental DSC data to a two-state model, data trimming is manifested by folded and unfolded baselines that cross at temperatures close to the transition region. Crossing of folded and unfolded baselines has been reported for a leucine zipper by Dragan and Privalov (*37*), for apoflavodoxin by Irun et al. (*41*), and for Naf-BBL by us (*21*). In all cases, this result was seen as a clear indication that the unfolding transition is not two-state. In Figure 3C, we show the fitting of QNND-BBL's DSC thermogram to the simplest two-state model (i.e., assuming that ΔH and ΔS are constant within the transition region) with $\Delta H_m = 129$ kJ/mol and $T_m = 329$ K. This fit, which enforces a $\Delta H_{cal}/\Delta H_{vH}$ of unity, is very good. However, the native and unfolded baselines cross at a temperature that is in the middle of the unfolding transition (see the fitted baselines in Figure 3C). Such result is unphysical because it implies that ΔC_p reaches unrealistically large values at low temperatures and changes sign in the middle of the unfolding transition. Indeed, a simple calculation of the DSC thermogram with those parameters, but now taking into account ΔC_p as obtained from the difference

between the two straight baselines, predicts a significant degree of cold-denaturation at 285 K which is not experimentally observed (see dotted line in Figure 3C). The fitting to a two-state model can be done successfully with other approximations, including fits in which ΔC_p is directly calculated from the baselines. The latter is greatly facilitated by assuming that the unfolded state C_p changes nonlinearly with temperature, as suggested by model compounds (*33*), and has been done with other small proteins (*42*). However, in all instances, the two fitted baselines of QNND-BBL cross within the transition region (data not shown). Therefore, the DSC data indicate that QNND-BBL is not a two-state folder. This conclusion is independent of the possible existence of low-temperature artifacts in these data (see next section). The reason is that such an artifact lowers the low-temperature baseline leading to an underestimation of the degree of baseline crossing.

Fersht and co-workers also introduce nuclear magnetic resonance (NMR) data for QNND-BBL. Particularly, in their manuscript, they show the ^{13}C chemical shift as a function of temperature of the Cα or Cβ of six different residues in the protein. This is a powerful experiment for determining whether the inherent structural heterogeneity of downhill folding is polarized in structural subdomains. $^{13}C\alpha$ and $^{13}C\beta$ chemical shifts are temperature independent and mostly sensitive to the local conformation of the residue (*43*). In principle, the experiment can provide a very large number of local probes that are measured simultaneously, at exactly the same temperatures and in the same sample. Errors in the determination of temperature and other slight changes in experimental conditions propagate to all of the data and cancel out in the comparison between unfolding curves. Interestingly, Fersht and co-workers find that the thermodynamic parameters obtained by fitting each of the six unfolding curves to a two-state model vary (i.e., ΔH_m varying from 92 to 134 kJ/mol and T_m varying from 324 to 329 K (see Table 1 in ref *2*)). They interpret these sizable differences as a byproduct of experimental noise propagating into uncertainty in the fitted parameters.

The validity of this explanation can be easily investigated. As we discussed above, the only error that is relevant in comparing these six curves concerns the error in the determination of the chemical shift values, which essentially depends on the spectral resolution. An estimate from the fitting residuals indicates that this error is between 1% and 2% of the total amplitude of the unfolding curve (it is relatively larger for probes with a smaller change in chemical shift upon unfolding). If this error is the source of the parameter discrepancies, the deviations between normalized experimental points and fit for one probe should be similar in magnitude to the differences between normalized data at the same temperature from different probes. Figure 3E shows the normalized chemical shifts versus temperature of three of the six probes (L139, I149, and E161, keeping Fersht and co-workers nomenclature (*2*)). For clarity, the other three curves are not shown. Their values are within the spread of the ones shown here (curves for E161 and E164 have 100% correlated experimental noise and very similar chemical shifts, perhaps indicating that they have been obtained from two signals overlapping into one peak). Visual inspection of Figure 3E immediately suggests that the differences between probes are much larger than the experimental noise. Furthermore, the deviations between probes display very apparent trends. For example, each of the 12 points corresponding to the unfolding transition of Cα I149 is consistently ~6 K lower than the equivalent point of Cβ L139. To quantify the differences between thermodynamic behaviors of the various probes, we used the analysis described in the previous section for comparing Naf-BBL and Naf-BBL-Dan. The idea is to investigate the compatibility between the data for one probe and the thermodynamic parameters obtained for other probes. Thus, we fitted each unfolding curve to a series of two-state models in which the baselines floated while ΔH_m and T_m were fixed to the values corresponding to each of the other probes (obtained in unconstrained fits). The SLS of the constrained fits was 5.5 ± 1.9 times higher than the SLS of the unconstrained fit. We determined that, for random noise of the magnitude present in the data, the SLS of the constrained fits should increase only 0.2 times. Therefore, the probability that the NMR probes analyzed by Fersht and co-workers share the same unfolding behavior is statistically negligible.

Once established that the various probes exhibit different thermodynamic properties, it is appropriate to examine the implications. Figure 3F shows the native probability for the three probes of Figure 3E as calculated from their individual two-state fits. The figure reveals distinct unfolding behaviors, with individual residues unfolding at different temperatures and with different slopes. Although the available data is too scarce for a detailed analysis, there are hints of structural polarization. In particular, probes monitoring the structured loop (Cβ N143, Cα I149) and hydrophobic core (Cβ L139) have significantly lower sensitivity to temperature (smaller ΔH) than those monitoring the integrity of the two helices (Cα R136, Cα E 161, Cα E164). This is an interesting observation because a downhill folding transition could still produce very similar unfolding curves in this experiment. The reason is that ^{13}C chemical shifts are mainly sensitive to the local conformation of the residue. For individual local probes, the effects of a broad ensemble of conformations with decreasing degree of nativeness tend to average out, unless there is regional polarization in the ensemble. The fact that the six probes show significant differences suggests that the conformational heterogeneity of QNND-BBL is polarized in regions to some degree.

Tail Effects: Ac-Naf-BBL-NH_2 and QNND-BBL Have the Same Thermodynamic Properties. The analysis described in the previous section indicates that QNND-BBL is not a two-state folder. Rather, QNND-BBL appears to share the folding behavior of Naf-BBL and Naf-BBL-Dan. Despite the overall similarity, the experiments reported by Fersht and co-workers on QNND-BBL do show that this protein is slightly more stable than our variants. The apparent T_m measured by CD and DSC is ~7−10 K higher for QNND-BBL, which amounts to ~4 kJ/mol increased stability at 298 K when determined with a two-state model. Fersht and co-workers propose two possible explanations for the difference in stability: (i) either of the two fluorescence probes introduced by us interacts with the protein perturbing its folding and (ii) the lack of the QNND N-terminal tail in our constructs could have deleted important native interactions. The second explanation is unlikely because the N-terminal tail is totally unstructured in the native protein, as judged from the original NMR structure (*22*) and also confirmed by Fersht and co-

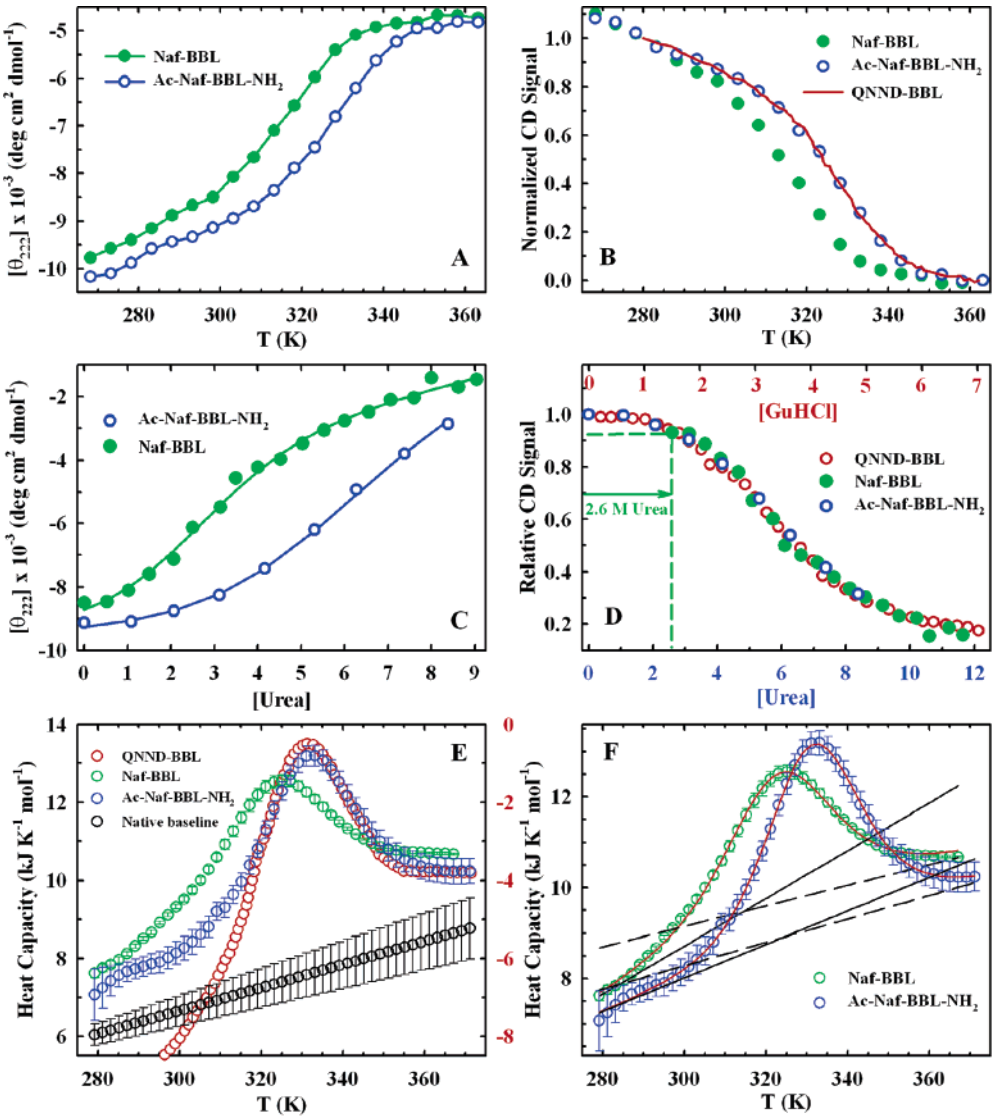

FIGURE 4: (A) Thermal unfolding transition of Naf-BBL and Ac-Naf-BBL-NH_2 monitored by CD at 222 nm. (B) Normalized thermal unfolding transition of Naf-BBL and Ac-Naf-BBL-NH_2; together the normalized thermal unfolding transition of QNND-BBL obtained by Fersht and co-workers (*2*). (C) Urea denaturation at 298 K of Naf-BBL and Ac-Naf-BBL-NH_2 monitored by CD at 222 nm. The continuous lines are individual fits to a two-state model. (D) Superimposition of urea-induced unfolding data of Naf-BBL (green filled circles, lower scale shifted 2.6 M urea) and Ac-Naf-BBL-NH_2 (open blue circles, lower scale) and GuHCl-induced unfolding data of QNND-BBL (open red circles, upper scale). The data for Naf-BBL and Ac-Naf-BBL-NH_2 is shown relative to the Ac-Naf-BBL-NH_2 signal at 0 M urea. The data for QNND-BBL has been taken directly from ref *2*. (E) DSC thermograms of Naf-BBL and Ac-Naf-BBL-NH_2 together with the thermogram for QNND-BBL obtained by Fersht and co-workers (*2*). The black open circles correspond to the native baseline calculated from Freire's equation (*50*). (F) Two-state fits (continuous red lines) to the DSC thermograms of Naf-BBL and Ac-Naf-BBL-NH_2. Native (continuous black lines) and unfolded (dashed black lines) fitting baselines are shown for both proteins.

workers (*2*). The C-terminal dansyl of the doubly labeled BBL can also be excluded because it is not present in Naf-BBL and does not modify the folding of BBL when introduced in Naf-BBL-Dan (see first section and ref *1*). The remaining possibility (i.e., the N-terminal naphthyl-alanine) is favored by Fersht and co-workers, who argue that, in their newly determined structure, the substituted alanine forms the edge of the hydrophobic core (*2*). One available piece of evidence against this interpretation is the fact that the quantum yield of Naf-BBL is identical to that of free naphthyl-alanine (*29*).

Another possible explanation is that the lower stability of Naf-BBL and Naf-BBL-Dan results from repulsive interactions between the charged ends and the helix macrodipole. This interaction is especially strong at the N-terminus and decays quickly with the sequence separation between the charge and the start of the helix (*44*). In Naf-BBL, the N-terminal charge is two residues from the N-cap of helix 1, while in QNND-BBL, is separated by four additional residues. To experimentally determine which interpretation is more plausible, we analyzed a variant of BBL labeled at the N-terminal with naphthylalanine and in which the end charges have been eliminated by acetylation and amidation (i.e., Ac-Naf-BBL-NH_2). In discussing the data introduced in this section, we make ample use of two-state analyses and analogies. We use them with the intention of facilitating data comparison and/or illustrating potential problems.

Figure 4A shows the mean residue ellipiticity at 222 nm of Ac-Naf-BBL-NH_2 and Naf-BBL as a function of temperature. The CD222 unfolding curve of Ac-Naf-BBL-NH_2 has pre- and post-transition slopes that are very similar to those of Naf-BBL, but the main transition is shifted by ~9

K. The mean residue ellipticity of Ac-Naf-BBL-NH_2 is more negative at the lowest temperatures and also slightly more negative in the posttransition. More negative ellipticity values at 222 nm suggest an increase in the α-helix content. The increase is even more pronounced if we consider that Ac-Naf-BBL-NH_2 has two additional, intrinsically disordered, peptide bonds. This is an interesting point because the increase in α-helix signal is most evident in the low-temperature region, which would be classified as the pretransition in a standard two-state analysis. In fact, the CD signal for the two proteins superimpose after shifting their temperature scales by 9 K. The implication is that the folding ensemble of BBL is plastic and increases its nativeness as the energy gradient becomes more favorable. Such observation also emphasizes the importance of reporting the spectroscopic signal in absolute units. Any kind of normalization procedure eliminates this piece of evidence and makes the experimental data look more two-state-like.

Unfortunately, direct comparison with the currently available CD data on QNND-BBL requires normalization. In addition, the experiments on QNND-BBL have been carried out at higher ionic strength (i.e., 200 versus 20 mM phosphate). However, we have determined that the thermodynamic properties of Naf-BBL and Ac-Naf-BBL-NH_2 are not significantly affected by changes in ionic strength within that range. Fersht and co-workers also indicate that the thermodynamic properties of QNND-BBL are unaffected by ionic strength (*2*). Therefore, the normalized CD222 unfolding curve of the three proteins should still be directly comparable (Figure 4B). The normalization has been performed using the values at the highest and lowest common temperatures for the three datasets. It is evident from Figure 4B that the CD222 unfolding curves of Ac-Naf-BBL-NH_2 and QNND-BBL are identical. From the comparison in Figure 4B, it also appears that the three proteins share very similar thermal unfolding properties. A simplistic two-state analysis of these curves produces $\Delta H_m \sim 115$ kJ/mol for Ac-Naf-BBL-NH_2 and QNND-BBL and $\Delta H_m \sim 96$ kJ/mol for Naf-BBL. These numbers are surprisingly close to the values for 40−44 residue proteins extrapolated from the analysis of larger two-state proteins (*35*). Because ΔC_p is found to scale by ∼58 J/(mol·K) per residue and ΔH at 333 K by ∼2.92 kJ/mol per residue, this analysis predicts $\Delta H =$ 115 kJ/mol at 330 K (i.e., ∼ apparent T_m of Ac-Naf-BBL-NH_2 and QNND-BBL) and $\Delta H = 93$ kJ/mol at 321 K (i.e., ∼ apparent T_m of Naf-BBL). Once more, a simple calculation invalidates a previous assertion by Fersht and co-workers, in this case, claiming that the thermodynamic properties of Naf-BBL are inconsistent with those of other similar sized proteins (*2*). The fact that large two-state and small downhill folding proteins keep the same scaling of thermodynamic parameters is an interesting observation. It suggests that two-state and downhill are just extreme scenarios of a general phenomenon in which the height of the folding barrier is modulated by conditions, such as the size of the protein. The recent observation of strong correlation between folding rate and protein size (*45*, *46*) provides further empirical support to this notion. The general concept is, of course, at the core of statistical mechanical treatments of protein folding (*5*, *8*−*10*, *12*, *13*, *47*).

Figure 4C shows the urea-induced unfolding of Naf-BBL and Ac-Naf-BBL-NH_2 at 298 K monitored by CD at 222 nm. The sensitivity to urea is quite low for both proteins, and neither transition is complete. Ac-Naf-BBL-NH_2 seems to still be within the transition region at 8.5 M urea. Naf-BBL reaches some kind of sloped post-transition baseline at high concentrations of urea. In water, Naf-BBL seems to be partially unstructured already (note that these conditions correspond to the end of the pretransition in the temperature denaturation experiment (Figure 4A)). The lines through the data correspond to independent two-state fits and are shown to guide the eye. At first sight, the two unfolding curves seem quite disparate. However, the curves of the two proteins superimpose when the data for Naf-BBL is shifted by 2.6 M urea (Figure 4D). Superimposing these two curves does not require any normalization, but Figure 4D displays the data divided by the total maximal signal (i.e., the value at 0 M urea of Ac-Naf-BBL-NH_2) to allow comparison with the available data on QNND-BBL. The fact that the curves of Naf-BBL and Ac-Naf-BBL-NH_2 superimpose indicates that the response to urea is the same for both proteins. Such assertion is confirmed by a simple analysis with two-state models. Fitting of the composite curve (the blue and green circles of Figure 4D) to a two-state model produces and apparent m value of ∼1.7 kJ/(mol·K) and $[\text{urea}]_{1/2}$ of ∼5.6 M. The individual two-state fits to the Naf-BBL data fixing the "native" baseline and to the Ac-Naf-BBL-NH_2 data fixing the "unfolded" state baseline, produce the same ∼1.7 kJ/(mol·M) m value and $[\text{urea}]_{1/2}$ values of ∼3 and ∼5.6 M, respectively. Because there is not enough information in each dataset to obtain the two baselines, the parameters obtained in fully unconstrained fits are inconsistent. The lack of a "native" baseline seems to be the source of the problems encountered by Fersht and co-workers in analyzing their chemical denaturation data on Naf-BBL-Dan (*2*). As illustrated here and by Felitsky and Record in their work on lac-repressor (*25*), such problems are eliminated with additional information on the expected baselines. It is also important to note that the composite curve of Naf-BBL and Ac-Naf-BBL-NH_2 can be superimposed to the GuHCl unfolding curve of QNND-BBL once the scales are corrected to reflect the different sensitivity to urea and GuHCl (see lower and upper scales in Figure 4D). From the superimposition, we find that the ratio between the sensitivity to GuHCl and to urea is ∼1.75. This ratio is well within the values observed for larger proteins (*48*). A similar ratio is obtained from independent two-state fits, which render ∼2.9 kJ/(mol·M) for the GuHCl unfolding of QNND-BBL versus ∼1.7 kJ/(mol·M) for the composite curve. When the apparent m value of the composite curve is used, the 2.6 M shift converts into ∼4.4 kJ/mol of destabilization for Naf-BBL versus Ac-Naf-BBL-NH_2. On the other hand, QNND-BBL and Ac-Naf-BBL-NH_2 have the same stability.

The comparison between the DSC data of the three proteins is shown in Figure 4E. This comparison is particularly relevant because DSC was the only piece of our original data on Naf-BBL (*1*) that Fersht and co-workers directly compared to their data on QNND-BBL (*2*). In all other instances, Fersht and co-workers compared QNND-BBL with their own data on Naf-BBL-Dan, which was obtained in aggregating conditions. The absolute heat capacities for Naf-BBL and Ac-Naf-BBL-NH_2 (Figure 4E) have been determined from the protein concentration dependence of the apparent heat capacity values (*49*). This procedure requires

several DSC experiments at different protein concentrations. Although time-consuming, this approach provides an accurate determination of the absolute heat capacity together with an estimate of the associated standard errors (see, for example, ref *24*). Figure 4E also shows the heat capacity expected for the native baseline of these proteins calculated with the empirical formula of Freire (*50*). The DSC thermogram of Naf-BBL has exactly the same properties discussed before (*1*, *21*). It is a very broad thermogram with a maximum at ~324 K and with a steep slope at low temperatures. Furthermore, at the lowest temperature, the heat capacity is still 1.5 kJ/(mol·K) higher than the native baseline, indicating the presence of large enthalpy fluctuations. The thermogram of Ac-Naf-BBL-NH_2 has a maximum at ~332 K. The peak is higher and sharper, as it corresponds to a protein unfolding transition that is shifted ~8 K up. With a higher T_m, the thermogram of Ac-Naf-BBL-NH_2 shows what appears to be a bona fide low-temperature baseline (280−300 K). Besides, both, the low- and the high-temperature baselines, have lower absolute heat capacities than their counterparts in Naf-BBL. The latter reflects more order and is consistent with our previous observation of increased α-helix content in Ac-Naf-BBL-NH_2 (see Figure 4A). The increased order is, however, still far from the expectation for a native protein, as reflected in a low-temperature baseline that is >1 kJ/(mol·K) higher than the predicted native baseline and with higher temperature dependence. It is important to note that the thermograms of the two proteins can be fitted to a two-state model. The fitting, performed enforcing a $\Delta H_{cal}/\Delta H_{vH}$ of unity and using the baselines to obtain the experimental ΔC_p, results in very low residuals for both proteins (Figure 4F). However, the fits are unphysical because the "native" and "unfolded" baselines cross in the middle of the transition, and the "native" baseline is too high and has too steep a temperature dependence. This calculation nicely illustrates that the magnitude of the fitting residuals and a $\Delta H_{cal}/\Delta H_{vH} = 1$ are not sufficient criteria for two-stateness. Furthermore, the almost parallel two-state baselines (see Figure 4F) and the matching ΔH_m values (Naf-BBL, ~100 kJ/mol at ~322 K; Ac-Naf-BBL-NH_2, ~125 kJ/mol at ~331 K) emphasize that these two proteins have slightly different stability but the same overall thermodynamic behavior.

The DSC thermogram of QNND-BBL measured by Fersht and co-workers is shown in red in Figure 4E. As we have discussed in the previous section, these data are not in absolute heat capacity units. Therefore, we display them keeping the original scale expressed in kJ/(mol·K) (right scale in Figure 4E) but shifting the origin to match the heat capacity values at the highest temperature with those of Ac-Naf-BBL-NH_2. The temperature of the maximum, the maximum height of the peak, and the broadness of the transition in the thermogram of QNND-BBL are very similar to those of Ac-Naf-BBL-NH_2's thermogram. The agreement indicates that these two proteins have the same thermodynamic properties, as we had concluded from the CD analysis. However, there is a striking difference at low temperatures. The thermogram of QNND-BBL shows an extremely pronounced tail that dips down to very low relative heat capacity values (reaches a value of −10 at 280 K). Not only is this tail much larger than the tail of Naf-BBL and Ac-Naf-BBL-NH_2, but it reaches values that are incompatible with the predicted native baseline (i.e., the relative heat capacity of

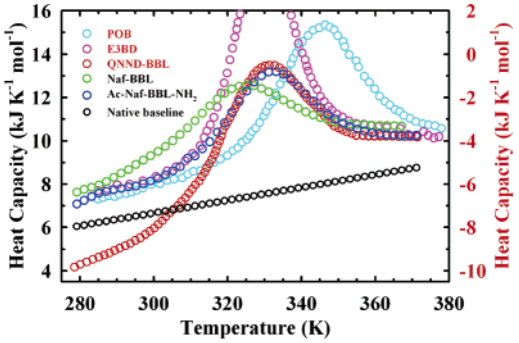

FIGURE 5: DSC thermograms of Naf-BBL and Ac-Naf-BBL-NH_2 (left scale) together with the DSC thermograms for QNND-BBL and the mutants of the two other BBL homologues (POB, E3BD) studied by Fersht and co-workers (*2*) (right scale). The black open circles correspond to the native baseline for BBL calculated from Freire's equation (*50*) (left scale). The scale of the plot has been chosen to facilitate the comparison of the low- and high-temperature baselines.

QNND-BBL at 280 K scales to ~2 kJ/(mol·K) below the expected native baseline). In fact, the difference in heat capacity between the highest and lowest temperatures in the thermogram of QNND-BBL is 6 kJ/(mol·K), while the ΔC_p expected for a protein of this size is 2.5 kJ/(mol·K) (*35*). Thus, it is evident that the thermogram of QNND-BBL has an artifact at low temperatures. It is quite surprising that Fersht and co-workers did not detect the presence of such artifact in their data. The insensitivity of Fersht and co-workers to the anomalous QNND-BBL thermogram is even more noteworthy given that they also measured the DSC of two homologous proteins, which show no signs of such tail (see Figure 2D in ref *2*). The anomaly becomes dramatically apparent in the comparison between the DSC data of the five proteins (see Figure 5). Such artifact could arise by insufficient calorimeter equilibration prior to the protein scan. One strategy to ensure that the calorimeter is properly equilibrated consists of measuring several invariant buffer−buffer baselines prior to the protein scan (see inset, Figure 2A). We routinely perform this test together with measurement of a buffer−buffer post-scan baseline to detect any significant instrumental drifts (inset in Figure 2A). These controls are particularly important when measuring DSC thermograms of small proteins with very broad unfolding transitions.

Ac-Naf-BBL-NH_2 Displays All of the Signatures of Downhill Folding. In the previous section we have established that Ac-Naf-BBL-NH_2 has the same thermodynamic stability than QNND-BBL. Here, we investigate the compliance of Ac-Naf-BBL-NH_2's thermodynamic properties with the different signatures that we have previously outlined for downhill folding (*1*, *20*, *21*). Figure 6A shows the temperature-induced unfolding of Ac-Naf-BBL-NH_2 monitored by far-UV CD at four diagnostic wavelengths. As we originally reported for Naf-BBL ((*20*), see Figure 3A), the apparent unfolding transition has significant wavelength dependence. The wavelength dependence reflects spectral changes that are already occurring during the pretransition and propagate throughout the transition region. The nature of these spectral changes suggests that the α-helices of BBL are detaching from one another and shortening progressively as temperature increases. Because each of the four chosen wavelengths is affected differently by the structural changes occurring in

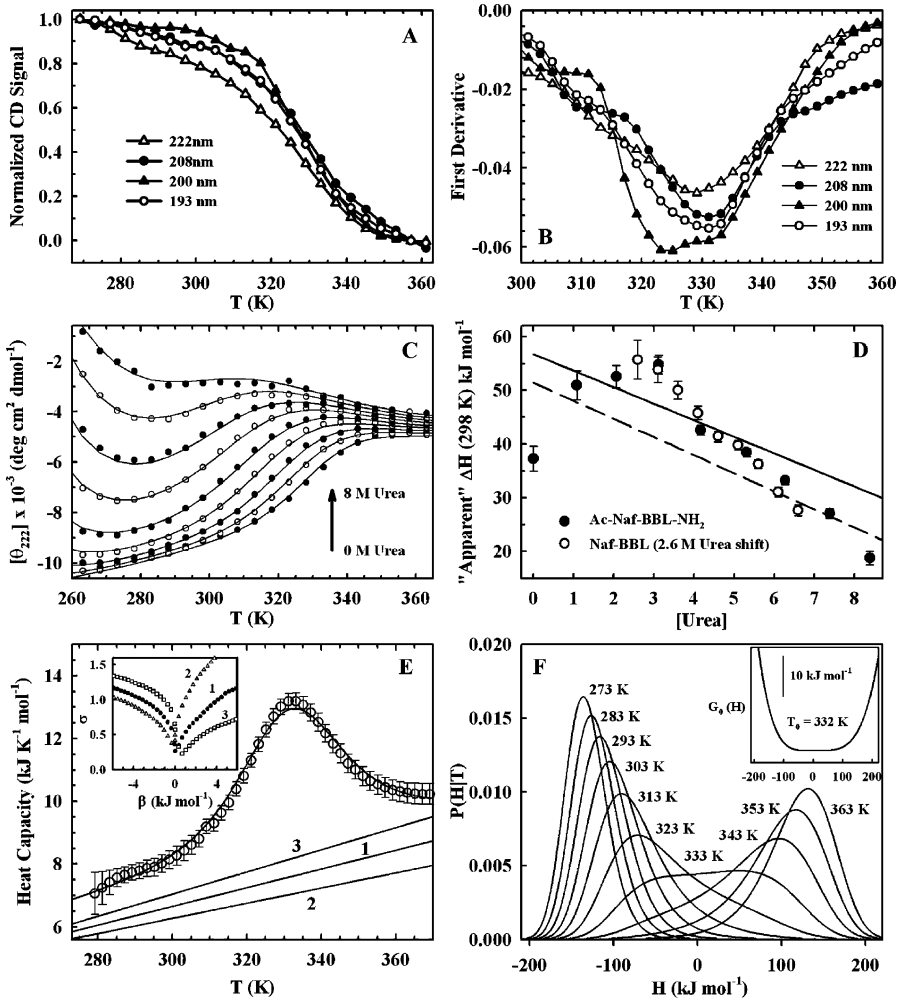

FIGURE 6: (A) Normalized thermal unfolding transitions of Ac-Naf-BBL-NH_2 monitored by CD at different wavelengths. (B) First derivative of the curves shown in panel A. (C) Equilibrium unfolding of Ac-Naf-BBL-NH_2 induced by temperature and urea (0−8 M urea in steps of 1 M) monitored by CD at 222 nm. The continuous lines correspond to a global-fit to a two-state model. (D) Urea dependence of the apparent ΔH for folding at 298 K obtained from individual two-state fits to the data shown in panel C; (continuous line) linear dependence for ΔH of folding at 298 K measured by Felitsky and Record in lac-repressor (*25*) and (dashed line) linear regression of the composite data for Naf-BBL and Ac-Naf-BBL-NH_2. (E) DSC of Ac-Naf-BBL-NH_2; (circles) data and (continuous line) fit to the variable-barrier model using baseline 1 (*50*). (inset) Plots of the standard deviation (in kJ K^{-1} mol^{-1}) versus the parameter β of the fits to the variable-barrier model using baselines 1 to 3. (F) Probability density of Ac-Naf-BBL-NH_2 as a function of temperature calculated from the fit of panel E. (inset) Free-energy profile at the characteristic temperature (T_0 = 332 K).

the α-helices of BBL, the thermal unfolding curves display different apparent T_m. This is most readily observed by calculating the derivative of the thermal unfolding curves (Figure 6B). The calculation produces apparent T_m values ranging from 326 K (200 nm) to 332 K (193 and 208 nm). Therefore, the CD data indicate that during the thermal equilibrium unfolding of Ac-Naf-BBL-NH_2, the α-helix structure changes continuously, as expected for a downhill folding transition.

Figure 6C shows a double perturbation experiment on Ac-Naf-BBL-NH_2, in which the coupling between temperature and urea is investigated monitoring the CD signal at 222 nm. The idea behind this test is simple. In a two-state transition, the properties of the ensemble at each condition are described by a linear combination between those of the folded and unfolded states (i.e., bimodal distribution). The thermodynamic parameters of the transition are defined by the difference between the values of the folded and unfolded states, and the coupling between different denaturing agents is determined by simple Maxwell relationships (*25*). The ensemble of a continuous (downhill) unfolding transition has a unimodal distribution that shifts its average properties from high to low degree of structure as the bias toward unfolding increases. Therefore, these two kinds of ensembles have very different second moments, but their first moments could be quite similar. Single perturbation experiments typically provide measurements of first moments (with the exception of DSC, see below) and thus, are insensitive to the main differences between the two scenarios. In fact, first-order, intermediate (i.e., transitions with barrier $<4RT$), and continuous transitions can all produce sigmoidal equilibrium unfolding curves (*20*). Sigmoidal unfolding curves can always be fitted to a chemical two-state model with unconstrained baselines regardless of the statistical nature of the transition. The classical approach to circumvent this limitation is to look for complex behavior by comparing the first moments of different structural properties (*1*, *19*). An alternative is to couple the effect of two denaturing agents with different mechanism of action (*20*). Each denaturant agent changes the properties of the ensemble in a particular way, thereby changing the response of the ensemble to the other denaturing agent. In the double perturbation experi-

ment, we observe for Ac-Naf-BBL-NH_2 the same behavior that we previously reported for Naf-BBL (*20*), with the only difference being that higher urea concentrations are required to induce the same degree of unfolding. The emergence of cold-denaturation, the very pronounced shift in the apparent T_{max} (i.e., the temperature of maximal "folded" signal) induced by urea, and the observation of pre- and post-transition slopes are all clearly apparent.

The continuous lines in Figure 6C correspond to a global two-state fit in which the dependence of ΔH and ΔS on urea are assumed linear. In this fit, the phenomenological baselines include slopes for temperature, for urea, and for the combined effect of both denaturing agents. The fitting procedure achieves a reasonable fit by choosing unphysical baselines for the folded and unfolded states (i.e., baseline crossing). Furthermore, although small, the differences between data and fit are systematic. As we reported in Naf-BBL (*20*), the global two-state model is unable to precisely reproduce the changes induced by urea in the ΔH_m and T_m of Ac-Naf-BBL-NH_2 (i.e., underpredicts the T_m at high and low urea and overpredicts it in the midrange, see Figure 6C). For a two-state transition, the effects of increasing urea concentrations on ΔH and ΔS are linear to a first-order approximation (*26*, *51*−*53*). Linear urea dependences of the basic thermodynamic parameters have been recently reported for the lac-repressor using the same kind of double perturbation experiment (*25*). In Ac-Naf-BBL-NH_2, the discrepancies between data and global two-state fit indicate that the coupling between temperature and urea is complex, as expected for a downhill folding protein. This conclusion is better illustrated by plotting the apparent ΔH at 298 K versus urea as obtained in individual two-state fits to the thermal unfolding transitions at different urea concentrations (Figure 6D). To facilitate convergence and maintain consistency, these individual fits have been performed keeping the folded baseline and the ΔC_p fixed to the values obtained in the global fit. Figure 6D shows a highly curved ΔH versus urea plot with a maximum between 2 and 3 M urea. The curvature of the ΔS versus urea plot is similar, while the plot for ΔG is S-shaped (data not shown). The ΔH versus urea plots for Ac-Naf-BBL-NH_2 and Naf-BBL overlay when the latter is shifted by 2.6 M urea, once again illustrating that the two proteins have different stability but behave the same way. The curvature of the apparent ΔH versus urea plot is a particularly powerful signature of downhill folding because it is only sensitive to the behavior in the region of steeper temperature dependence (i.e., the apparent transition region). Thus, this criterion could be particularly useful to distinguish between pure downhill and intermediate transitions with barriers $<4RT$. Intermediate transitions are characterized by the presence of structural changes in the pre- and/or post-transition regions and a main unfolding transition that deviates only slightly from classical two-state. It is also interesting to note that the magnitude of ΔH and its average urea dependence (dashed line in Figure 6D) are very similar to the ΔH versus urea line obtained by Felitsky and Record on the small α-helical protein lac-repressor (continuous line in Figure 6D), which has been found compatible with a two-state transition (*25*). This observation further supports the concept that the two-state and downhill folding regimes do not originate in intrinsically different thermodynamic parameters.

Finally, we have analyzed the DSC thermogram of Ac-Naf-BBL-NH_2 with the recently developed variable-barrier model (*21*). One of the most special properties of the DSC data is that it is directly connected to the probability density of the system under study through the inverse Laplace transform of the partition function (see ref *54* for a discussion of this issue in the context of protein folding). The implication is that the DSC thermogram of a protein contains information about the shape of the probability distribution for unfolding and, therefore, about the presence or absence of a folding free-energy barrier. Taking advantage of this property, our variable-barrier model extracts the height of the folding barrier from the DSC thermogram using a simple free-energy functional with the general properties of the Landau Free Energy (*21*). The model only has four adjustable parameters, which determine the general properties of the folding ensemble: height of the barrier, shape and width of the one or two wells, and the enthalpy scale. Furthermore, it does not incorporate phenomenological baselines. The DSC data are analyzed after subtraction of the native baseline, and the excess heat capacity is directly calculated from the probability density. Therefore, the fitting to this model is highly constrained because baseline manipulation is minimized to avoid data trimming. The results of fitting this model to the thermogram of Ac-Naf-BBL-NH_2 are shown in Figure 6E. The fit shown in the figure corresponds to a native baseline estimated with Freire's empirical formula (baseline 1 in Figure 6E, black symbols in Figure 4E). Baselines 2 and 3 correspond to one standard deviation below and above, respectively (see Figure 4E). Despite its extreme simplicity and highly constrained nature, the model reproduces the experimental data quite well (i.e., residuals within experimental uncertainties). The parameters of the best fit are $\beta = 0$ kJ/mol, $\sum\alpha = 58$ kJ/mol, $f = 0.9$ at $T_0 = 332$ K. The parameter β determines the height of the barrier. Thus, the best fit to the model produces a barrierless unfolding transition. Furthermore, fits to baselines 2 and 3 also produce no barrier, or negligible barriers (i.e., $<RT$) (see inset of Figure 6E). Figure 6F shows the probability density at different temperatures calculated from the best fit to the model. The probability density is unimodal at all temperatures, shifts its maximum from low enthalpy to high enthalpy values at increasing temperature, and has the broadest distribution near T_0. All of these features agree precisely with the expectation for a downhill folding protein. The free-energy functional at T_0 (inset of Figure 5F) shows very clearly that the unfolding transition of Ac-Naf-BBL-NH_2 is barrierless.

We also applied the variable-barrier model to the DSC data obtained by Fersht and co-workers on QNND-BBL. Because the available data is not in absolute heat capacity units, we arbitrarily chose native baselines that coincided with the lowest temperature datapoint and with temperature dependences in the range of that predicted by Freire's empirical correlation (*36*). Such native baselines result in DSC thermograms for QNND-BBL that are as maximally two-state as is physically reasonable. Yet, all the fits to the variable-barrier model produced barrierless profiles (data not shown). Unfortunately, the quality of the best fits was always poor due to the low-temperature artifact mentioned in the previous section.

CONCLUSIONS

The energy landscape approach to protein folding categorizes the thermodynamic and kinetic behavior of proteins in various folding scenarios. The type 1 scenario corresponds to classical two-state folding, while the type 0 scenario represents barrierless folding (i.e., downhill folding) (*5*). Which of these two scenarios applies to a given folding transition is expected to depend on the properties of the protein and the specific environmental conditions. For many years, conventional wisdom has asserted that only the first scenario is relevant to natural single-domain proteins (*15*). Quite recently, we discovered that the small protein BBL folds downhill at all native biases (*1*), resulting in a continuous equilibrium unfolding transition. Using simple statistical mechanical arguments and this protein as model case, we have later developed additional procedures to distinguish between downhill and two-state folding (*20*, *21*). Although a natural concept in condensed matter physics, the idea that a protein with spectroscopically well-defined structure (i.e., an ordered phase) can unfold following a continuous transition has not been fully accepted among protein biochemists. Along these lines, Fersht and co-workers have recently published a paper in which they claim that a variant of BBL with no fluorescent labels and a longer N-terminal tail (QNND-BBL) folds as a two-state system and that our previous conclusions were based on aggregation artifacts, possibly induced by the presence of fluorescent labels in our protein variants (*2*).

Analyzing the experimental results of Fersht and co-workers on QNND-BBL, we find that their data are incompatible with a two-state transition. In addition, we show that Naf-BBL, the singly labeled variant of BBL that we used originally to obtain DSC and CD data (*1*), does not aggregate and folds reversibly by DSC. We also show that Naf-BBL-Dan, the doubly labeled BBL variant that we used for fluorescent measurements (*1*), does not aggregate and folds reversibly at the conditions used in the fluorescence experiments. Furthermore, when studied in nonaggregating conditions, Naf-BBL and Naf-BBL-Dan have the same thermodynamic properties. The implication is that the incorporation of the dansyl group at the C-terminus of BBL does not perturb its folding behavior. From the detailed analysis of a new variant of the singly labeled BBL in which both ends are chemically protected (Ac-Naf-BBL-NH_2) and its comparison with Naf-BBL and QNND-BBL, we conclude that the naphthyl-alanine at the N-terminus does not perturb the folding behavior of BBL either. Moreover, Ac-Naf-BBL-NH_2 has the same stability and thermodynamic properties of QNND-BBL and displays all of the signatures for global downhill folding that we have previously described (*1*, *20*, *21*). Therefore, global downhill folding is a robust property of the protein BBL that does not depend on the presence of fluorescent probes or on the stability of the protein. The downhill character of BBL is not a reflection of a drastic departure from the thermodynamic behavior of classical two-state proteins. Neither is downhill folding a consequence of the protein not having a spectroscopically defined structure. The protein BBL in its different forms has the NMR spectroscopic features that permit calculating high-resolution three-dimensional structures (*1*, *2*, *22*). The fact that the NMR data are consistent with a unique three-dimensional structure indicates that BBL variants are not molten globules. However, the ability to calculate a high-resolution three-dimensional structure from NMR data does not mean that the protein has a unique three-dimensional structure. It simply means that the average of all of the ensemble conformations is highly structured, although there might be large structural fluctuations in this ensamble (*55*). Our work suggests that two-state and global downhill are just the two extremes of a continuum spectrum of folding barrier heights, as originally predicted by theory (*5*). Which regime predominates seems to be determined by the interplay between several factors. One of them is the simple scaling of thermodynamic properties with protein size, which indicates that the smaller the protein, the lower the folding free energy barrier (*46*). Another emerging factor is the contribution to protein stability of many-body interactions. Polymer-chain models show that the larger the many-body contribution, the higher the free-energy barrier (*47*). This same idea has recently been invoked to rationalize that crude empirical estimates of the conformational entropy at the top of the barrier produce very similar values (i.e., $^2/_3$ of that of the unfolded state) for several two-state proteins (*16*). Like for any other thermodynamic property, the height of the barrier will also depend on environmental conditions and specific features of protein structure and sequence (*17*, *18*).

An interesting side effect of the controversy originated by our downhill folding work is that it provides a unique opportunity to reevaluate methods and procedures in protein folding. Traditionally, the assessment of whether the equilibrium unfolding transition of a protein is first-order or not has been based on the individual fitting of unfolding curves to a chemical two-state model. The typical criterion for two-stateness is the agreement between thermodynamic parameters derived from curves measured with different techniques and/or between parameters measured directly and obtained assuming a pseudo-two-state model (i.e., the $\Delta H_{cal}/\Delta H_{vH}$ ratio). While this criterion can be effectively used to rule out two-state behavior, its apparent compliance with experimental data *is not proof* that the protein folds as a two-state system (*39*, *40*). This is particularly true for small proteins, which tend to have broad unfolding transitions accompanied by a high degree of uncertainty in baseline determination. Ultimately, such criterion supports a two-state transition only to the extent allowed by the quality of the data and analysis. Because everything can look alike in a blurred image, it is critical to interpret the spectroscopic signals, to check the feasibility of the fitted baselines, and to compare data directly. Sometimes neither of these things has been done before concluding that a protein folds in a two-state manner. The recent work of Fersht and co-workers (*2*) is a paradigmatic example of such extreme case. In their work, the CD and DSC data is shown either normalized or in relative units so that the information on the properties of the ensemble is lost. The experimental and fitting baselines, which are inconsistent with a two-state transition, are ignored. The CD unfolding transition is measured at several wavelengths, but all of them correspond to the same α-helix band (i.e., they monitor exactly the same spectroscopic feature). The fact that the two-state fit to the DSC data is unphysical is not addressed. No global fit is performed to see to what extent the whole dataset is compatible with a unique set of thermodynamic parameters. Instead, the deviations of the

parameters obtained in individual two-state fits are arbitrarily classified as due to experimental uncertainty. Errors in the two-state fits are also used to justify ^{13}C chemical shift unfolding curves that differ from one another. This is argued even though in all these curves the experimental errors propagate exactly the same way; their differences have very apparent trends and are much larger than the fluctuations in each individual curve. In summary, the work of Fersht and co-workers on BBL offers an impressive catalog of the potential problems and limitations of the traditional analysis of equilibrium protein folding transitions. This is hardly surprising. Such procedures were originally developed to distinguish between two-state and three-state chemical models and not to discriminate between first-order and continuous unfolding transitions. In recent years, there has been an increasing interest in investigating the folding of small fast-folding proteins (*56*, *57*). Obviously, these proteins are expected to have very small folding barriers (*57*) and, thus, should have equilibrium transitions ranging from marginally first-order to fully continuous. For all these proteins, a "chemical" view of protein folding is inappropriate, and the conventional methods of analysis are insufficient. At first, this realization may seem discouraging. In our view, it is an exciting development. The implication is that there is a lot of mechanistic information to be directly extracted from these small proteins by experiment. However, to fully achieve this promise may require that more experimentalists shift their paradigm into a more physical description of protein folding.

ACKNOWLEDGMENT

V.M. is recipient of a Dreyfus New Faculty Award, a Packard Fellowship for Science and Engineering, and a Searle Scholarship. The research described in this article has been funded by National Institutes of Health Grant RO1 GM06680-01 and National Science Foundation Grant MCB0317294 (to V.M.) and Spanish Ministry of Education and Science Grant BIO2003-02229 and Feder Funds (to J.M.S.-R.).

REFERENCES

1. Garcia-Mira, M. M., Sadqi, M., Fischer, N., Sanchez-Ruiz, J. M., and Muñoz, V. (2002) Experimental identification of downhill protein folding, *Science 298*, 2191−2195.
2. Ferguson, N., Schartau, P. J., Sharpe, T. D., Sato, S., and Fersht, A. R. (2004) One-state downhill versus conventional protein folding, *J. Mol. Biol. 344*, 295−301.
3. Levinthal, C. (1968) Are there pathways for protein folding?, *J. Chim. Phys. Phys.-Chim. Biol. 65*, 44.
4. Zwanzig, R., Szabo, A., and Bagchi, B. (1992) Levinthals paradox, *Proc. Natl. Acad. Sci.U.S.A. 89*, 20−22.
5. Bryngelson, J. D., Onuchic, J. N., Socci, N. D., and Wolynes, P. G. (1995) Funnels, pathways, and the energy landscape of protein-folding−a synthesis, *Proteins: Struct., Funct., Genet. 21*, 167−195.
6. Hinds, D. A., and Levitt, M. (1995) Simulation of protein-folding pathways−lost in (conformational) space, *Trends Biotechnol. 13*, 23−27.
7. Dill, K. A., and Chan, H. S. (1997) From Levinthal to pathways to funnels, *Nat. Struct. Biol. 4*, 10−19.
8. Onuchic, J. N., LutheySchulten, Z., and Wolynes, P. G. (1997) Theory of protein folding: the energy landscape perspective, *Annu. Rev. Phys. Chem. 48*, 545−600.
9. Shakhnovich, E. I. (1997) Theoretical studies of protein-folding thermodynamics and kinetics, *Curr. Opin. Struct. Biol. 7*, 29−40.
10. Veitshans, T., Klimov, D., and Thirumalai, D. (1997) Protein folding kinetics: Timescales, pathways and energy landscapes in terms of sequence-dependent properties, *Folding Des. 2*, 1−22.
11. Dobson, C. M., Sali, A., and Karplus, M. (1998) Protein folding: a perspective from theory and experiment, *Angew. Chem., Int. Ed. 37*, 868−893.
12. Pande, V. S., Grosberg, A. Y., Tanaka, T., and Rokhsar, D. S. (1998) Pathways for protein folding: is a new view needed?, *Curr. Opin.Struct. Biol. 8*, 68−79.
13. Thirumalai, D., and Klimov, D. K. (1999) Deciphering the timescales and mechanisms of protein folding using minimal off-lattice models, *Curr. Opin. Struct. Biol. 9*, 197−207.
14. Chan, H. S., and Dill, K. A. (1998) Protein folding in the landscape perspective: chevron plots and non-Arrhenius kinetics, *Proteins; Struct., Funct., Genet. 30*, 2−33.
15. Jackson, S. E. (1998) How do small single-domain proteins fold?, *Folding Des. 3*, R81−R91.
16. Akmal, A., and Muñoz, V. (2004) The nature of the free energy barrier to two-state folding, *Proteins: Struct., Funct., Bioinf. 57*, 142−152.
17. Yang, W. Y., and Gruebele, M. (2003) Folding at the speed limit, *Nature 423*, 193−197.
18. Yang, W. Y., and Gruebele, M. (2004) Folding λ-repressor at its speed limit, *Biophys. J. 87*, 596−608.
19. Muñoz, V. (2002) Thermodynamics and kinetics of downhill protein folding investigated with a simple statistical mechanical model, *Int. J. Quantum Chem. 90*, 1522−1528.
20. Oliva, F. Y., and Muñoz, V. (2004) A simple thermodynamic test to discriminate between two-state and downhill folding, *J. Am. Chem. Soc. 126*, 8596−8597.
21. Muñoz, V., and Sanchez-Ruiz, J. M. (2004) Exploring protein folding ensembles: a variable barrier model for the analysis of equilibrium unfolding experiments, *Proc. Natl. Acad. Sci. U.S.A. 101*, 17646−17651.
22. Robien, M. A., Clore, G. M., Omichinski, J. G., Perham, R. N., Appella, E., Sakaguchi, K., and Gronenborn, A. M. (1992) 3-Dimensional solution structure of the E3-binding domain of the dihydrolipoamide succinyl transferase core from the 2-oxoglutarate dehydrogenase multienzyme complex of *Escherichia coli*, *Biochemistry 31*, 3463−3471.
23. Knott, M., and Chan, H. S. (2004) Exploring the effects of hydrogen bonding and hydrophobic interactions on the foldability and cooperativity of helical proteins using a simplified atomic model, *Chem. Phys. 307*, 187−199.
24. Guzman-Casado, M., Parody-Morreale, A., Robic, S., Marqusee, S., and Sanchez-Ruiz, J. M. (2003) Energetic evidence for formation of a pH-dependent hydrophobic cluster in the denatured state of *Thermus thermophilus* ribonuclease H, *J. Mol. Biol. 329*, 731−743.
25. Felitsky, D. J., and Record, M. T. (2003) Thermal and urea-induced unfolding of the marginally stable lac repressor DNA-binding domain: a model system for analysis of solute effects on protein processes, *Biochemistry 42*, 2202−2217.
26. Schellman, J. A. (1994) The thermodynamics of solvent exchange, *Biopolymers 34*, 1015−1026.
27. Desai, U. R., Osterhout, J. J., and Klibanov, A. M. (1994) Protein-structure in the lyophilized state−a hydrogen isotope-exchange NMR-study with bovine pancreatic trypsin-inhibitor, *J. Am. Chem. Soc. 116*, 9420−9422.
28. Griebenow, K., and Klibanov, A. M. (1995) Lyophilization-induced reversible changes in the secondary structure of proteins, *Proc. Natl. Acad. Sci. U.S.A. 92*, 10969−10976.
29. Sadqi, M., Lapidus, L. J., and Munoz, V. (2003) How fast is protein hydrophobic collapse?, *Proc. Natl. Acad. Sci. U.S.A. 100*, 12117−12122.
30. Cantor, C. R., and Schimmel, P. R. (1980) *Biophysical Chemistry*, Vol. II, W. H. Freeman and Company, New York.
31. Chen, Y. H., Yang, J. T., and Chau, K. H. (1974) Determination of helix and beta-form of proteins in aqueous-solution by circular-dichroism, *Biochemistry 13*, 3350−3359.
32. Freire, E., Haynie, D. T., and Xie, D. (1993) Molecular-basis of cooperativity in protein-folding. 4. Core−a general cooperative folding model, *Proteins: Struct., Funct., Genet. 17*, 111−123.
33. Makhatadze, G. I., and Privalov, P. L. (1995) Energetics of protein structure, *Adv. Protein Chem. 47*, 307−425.
34. Sanchez-Ruiz, J. M. (1995) In *Subcellular Biochemistry* (Biswas, B. B. R., S., Ed.) pp 133−176, Plenum Press, New York.
35. Robertson, A. D., and Murphy, K. P. (1997) Protein structure and the energetics of protein stability, *Chem. Rev. 97*, 1251−1267.

36. Gomez, J., Hilser, V. J., Xie, D., and Freire, E. (1995) The heat-capacity of proteins, *Proteins: Struct., Funct. Genet. 22*, 404−412.
37. Dragan, A. I., and Privalov, P. L. (2002) Unfolding of a leucine zipper is not a simple two-state transition, *J. Mol. Biol. 321*, 891−908.
38. Jackson, W. M., and Brandts, J. F. (1970) Thermodynamics of protein denaturation. A calorimetric study of reversible denaturation of chymotrypsinogen and conclusions regarding accuracy of two-state approximation, *Biochemistry 9*, 2294−2301.
39. Zhou, Y. Q., Hall, C. K., and Karplus, M. (1999) The calorimetric criterion for a two-state process revisited, *Protein Sci. 8*, 1064−1074.
40. Kaya, H., and Chan, H. S. (2000) Polymer principles of protein calorimetric two-state cooperativity, *Proteins: Struct., Funct., Genet. 40*, 637−661.
41. Irun, M. P., Garcia-Mira, M. M., Sanchez-Ruiz, J. M., and Sancho, J. (2001) Native hydrogen bonds in a molten globule: the apoflavodoxin thermal intermediate, *J. Mol. Biol. 306*, 877−888.
42. Viguera, A. R., Martinez, J. C., Filimonov, V. V., Mateo, P. L., and Serrano, L. (1994) Thermodynamic and kinetic-analysis of the SH3 domain of spectrin shows a two-state folding transition, *Biochemistry 33*, 2142−2150.
43. Spera, S., and Bax, A. (1991) Empirical correlation between protein backbone conformation and C-alpha and C-beta C-13 nuclear-magnetic-resonance chemical-shifts, *J. Am. Chem. Soc. 113*, 5490−5492.
44. Muñoz, V., and Serrano, L. (1995) Elucidating the folding problem of helical peptides using empirical parameters. 2. Helix macrodipole effects and rational modification of the helical content of natural peptides, *J. Mol. Biol. 245*, 275−296.
45. Li, M. S., Klimov, D. K., and Thirumalai, D. (2004) Thermal denaturation and folding rates of single domain proteins: size matters, *Polymer 45*, 573−579.
46. Naganathan, A. N., and Muñoz, V. (2005) Scaling of folding times with protein size, *J. Am. Chem. Soc. 127*, 480−481.
47. Chan, H. S., Shimizu, S., and Kaya, H. (2004) Cooperativity principles in protein folding, *Methods Enzymol. 380*, 350−379.
48. Myers, J. K., Pace, C. N., and Scholtz, J. M. (1995) Denaturant M-values and heat-capacity changes—relation to changes in accessible surface-areas of protein unfolding, *Protein Sci. 4*, 2138−2148.
49. Kholodenko, V., and Freire, E. (1999) A simple method to measure the absolute heat capacity of proteins, *Anal. Biochem. 270*, 336−338.
50. Freire, E. (1995) *Protein Stability and Folding*, Humana Press, Totowa, NJ.
51. Aune, K. C., and Tanford, C. (1969) Thermodynamics of denaturation of lysozyme by guanidine hydrochloride. 2. Dependence on denaturant concentration at 25 Degrees, *Biochemistry 8*, 4586−4590.
52. Knapp, J. A., and Pace, C. N. (1974) Guanidine-hydrochloride and acid denaturation of horse, cow, and *Candida krusei* cytochromes-c, *Biochemistry 13*, 1289−1294.
53. Scholtz, J. M., Barrick, D., York, E. J., Stewart, J. M., and Baldwin, R. L. (1995) Urea unfolding of peptide helices as a model for interpreting protein unfolding, *Proc. Natl. Acad. Sci. U.S.A. 92*, 185−189.
54. Chan, H. S. (2000) Modeling protein density of states: additive hydrophobic effects are insufficient for calorimetric two-state cooperativity, *Proteins: Struct., Funct., Genet. 40*, 543−571.
55. Zagrovic, B., Snow, C. D., Khaliq, S., Shirts, M. R., and Pande, V. S. (2002) Native-like mean structure in the unfolded ensemble of small proteins, *J. Mol. Biol. 323*, 153−164.
56. Ferguson, N., and Fersht, A. R. (2003) Early events in protein folding, *Curr. Opin. Struct. Biol. 13*, 75−81.
57. Kubelka, J., Hofrichter, J., and Eaton, W. A. (2004) The protein folding 'speed limit', *Curr. Opin. Struct. Biol. 14*, 76−88.

BI050118Y